UNIVERSIDADE FEDERAL DE JUIZ DE FORA
INSTITUTO DE CIÊNCIAS BIOLÓGICAS
POS GRADUAÇÃO EM CIÊNCIAS BIOLÓGICAS
IMUNOLOGIA E DIP

Lúcia Mara Januário dos Anjos

MODULATION OF IMMUNE RESPONSE TO INDUCED-ARTHRITIS BY LOW-LEVEL LASER THERAPY

Tese de Doutorado do Curso de Pós Graduação em Ciências Biológicas: Área: Imunologia e Doenças Infecto Parasitárias.

Juiz de Fora, 2018

Abstract

Once the Low-level laser therapy immune cells response are not always clarified, this study aimed evaluate the profile of cytokines and immune cells after LLLT on arthritis-induced model. Arthritis was induced in the C57BL/6 mice divided into five groups: untreated; dexamethasone treated; LLLT at 3 Jcm^{-2}; LLLT at 30 Jcm^{-2}; euthanized 5 hours after inflammation induction. Cytokines measurements by ELISA and mRNA cytokine relative levels by qRT-PCR were performed with arthritic ankle (IL-1β, lL-6, TNF-α, lL-10 and TGF-β). Macrophages, dendritic cells, natural killer cells, lymphocytes $CD4^+$, $CD8^+$, Treg and costimulatory proteins were quantified in the proximal lymph node by flow cytometry. Data showed a decrease in all cytokines levels after LLLT and alteration in its mRNA relative levels, differently depending on the energy density used. LLLT at 3 Jcm^{-2} showed an increase for all cells populations analyzed in lymph node as well as the costimulatory proteins expression on macrophages and dendritic cells. Additionally, enrichment on Treg population expressing higher levels of CD25 was observed. LLLT at 30 Jcm^{-2} showed increase of $CD8^+$ cells population. Besides an anti-inflammmatory cytokine profile at inflammation site LLLT induces changes on immune cells populations of proximal lymph node favoring the anti-inflammatory microenvironment through Treg enrichment.

Keywords: Low-level laser therapy; arthritis; cytokines; immune cells; Treg cells.

Introduction

Rheumatoid Arthritis (RA) is an inflammatory autoimmune disease characterized by chronic degeneration of the synovial joints. Tending to worsen over time as joint architecture is modify by synovitis (inflammation of the synovial membrane) the RA commonly is associated with pain and functional disability, systemic complications, early death, and important economic burden worldwide (CROSS et al., 2014; IDE et al., 2011). Genetic and environmental factors compound the disease etiology and the pathologic process involves disruption of the innate and adaptive immunity mechanisms, with production of autoantibodies, as well as migration T and B cells into the synovial compartment and subsequent chronic inflammation (BURMESTER et al. 2012; MAHDI et al., 2009)

The trigger event of RA seems to be the activation of the innate immune response, which includes the arthritis-associated antigens presentation (exogenous material and autologous antigens) through major histocompatibility complex (MHC) and costimulatory proteins as CD80/CD86 by dendritic cells, macrophages and activated B cells to T cells, which promote its differentiation mainly into T helper 1 (Th1) and Th17 cells phenotype. T- and B-cell activation mediate effector function in RA through the release of cytokines and chemokines, activation of leukocyte, macrophages, fibroblast and endothelial cells, moreover through help provision to B cells and, in the case of $CD8^+$ effector T cells, improvement of its cytotoxic activity (CHOY, 2012; MCINNES & SCHETT 2011).

Additionally, polymorphonuclear cells (PMN), mobilized by the chemokines and cytokines, infiltrate the synovial compartment and produce a wide range of pro-inflammatory cytokines, leading to increase in cell proliferation, vasodilatation, vascular permeability, and proteolytic enzymes secretion (e.g., matrix metalloproteinases - MMPs) from stromal cells of the synovium and from chondrocytes. MMPs (particularly MMP-1, 3, 8, 13, 14 and 16) promotes collagen type II degradation, altering the glycosaminoglycan composition and water retention capacity of joint cartilage, which results in joint

biochemical and mechanical dysfunctions (MCINNES & SCHETT 2011; SABEH et al., 2010).

Macrophages present a important role in RA degenerative progress due to its antigen presentation and osteoclastogenesis activities and as the major source of the pro-inflammatory cytokines TNF-a, IL-1 and IL-6. The TNF-α promotes stimulation of other cytokines expression such as IL-1β, induces also monocyte cytokine and protaglandin release, PMN activation, apoptosis and oxidative burst, besides decreases synovial fibroblast proliferation and collagen synthesis. IL-1β increase cytokine and chemokine release of synovial fibroblast and up-regulates the cell adhesion molecules expression in endothelial cells. IL-1β and TNF-α also stimulate the release of MMPs and IL-6 production, and the latter in turn promotes T-cell and B-cell proliferation and antibody production, haematopoiesis and thrombopoiesis induction (MCINNES & SCHETT, 2007; NISHIMOTO & KISHIMOTO, 2006; SZEKANECZ et al., 2009).

On the other hand the joint inflammation can be modulate by immunosuppressive activity of regulatory T (Treg) cells. Treg cells immune suppression mechanisms comprise secretion of cytokines, such as TGF-β and IL-10, direct cytotoxicity to activated effector T cells through secretion of perforin and granzyme A, inactivation of effectors T cells via cell surface immunosuppressive molecules, such as cytotoxic T lymphocyte antigen 4 (CTLA4) and Fas ligand. Moreover, Treg cell can inhibit DC maturation and promote downregulation of CD80/CD86 expression and competition with effector $CD4^+$ cells for interaction with antigen-captured antigen-presenting cells (HAQUE et al., 2014).

IL-10, produced also by B cells, can inhibit T-cell cytokine release and promotes its anergy, can induces Treg cells maturation, decrease dendritic cells activation and cytokine release as well as decrease synovial fibroblast MMP and collagen release. More, IL-10 inhibits proteases, upregulate Interleukin 1 receptor antagonist (IL-1Ra) and the metallopeptidase inhibitor (TIMP) production. TGF-β, produced also by synovial-fibroblast, offers ambivalent inflammatory effects in synovitis depending on the presence or absence of IL-6: in the presence can promote cells differentiation into Th17 cells and in the

absence of IL-6 it can favors a regulatory phenotype (Treg) of the T cells (ASIF AMIN et al., 2017; FIRESTEIN, 2003; MCINNES & SCHETT, 2007).

In spite of fibroblast-like synoviocytes (FLS), macrophages and T lymphocytes are the most abundant cell types in RA synovium and PMN are often the most abundant cellular component in the synovial fluid, neutrophils, mast cells, dendritic cells, natural killer (NK) cells, NKT cells, B cells, osteoclasts and plasma cells have been identified in the synovial compartments and present important role in the pathogenesis of RA through cytokines, chemokines, and proteases production, antigen presentation and production of antibodies, among others (ASIF AMIN et al., 2017; FIRESTEIN, 2003).

Once synovitis is the mainly clinical feature of RA, its therapy have been focused on inflammation modulation and consequently disease degenerative progression deceleration by administration of anti-inflammatory drugs (NSAIDs), corticosteroids, drugs modifying the course of the disease (DMARDs) synthetic and biological and immunosuppressive drugs, used alone or in combination. However, the treatment has several important side effects, especially in the administration of NSAIDs and corticosteroids, and sometimes does not show clinical improvement and disease remission (KIELY et al., 2009; SMOLEN et al., 2017), therefore a great deal of effort has been invested to identify other treatment strategies that present an anti-inflammatory effect but not suppress the entire immune system (CHOY, 2012). In this context, the low-level laser therapy (LLLT) could be considered a promising non-pharmacological alternative to RA treatment due to its local effects of tissue healing stimulation, inflammatory process modulation and pain relief (BROSSEAU et al., 2010; ANJOS et al., 2017; KAZEM SHAKOURi et al., 2010; KINGSLEY, 2014).

Despite the well-known anti-inflammatory effect of LLLT and its extensive clinical use in the treatment of chronic inflammatory conditions, the impact of this treatment on the components of the immune response to arthritis is still poorly explored. Keeping this in mind our research group investigated the immune response alterations after LLLT using an experimental arthritis-induced model (ASQUITH et al., 2009), evaluating cytokines levels at inflammation site and immune cells population profile in proximal lymph node to inflammation.

Material and Methods

Experimental groups and inflammatory process induction

Forty male C57BL/6 mice, 8-10 weeks old, weighting 24-28 g each were used (Animal Ethical Committee guidelines at Federal University of Juiz de Fora - protocol 039/2014), It was allowed to their move freely in the cages, had free access to laboratory diet and water the animals. The temperature (25° ± 2°C) and 12:12h light/dark cycles were controlled. The experimental animals were randomly distributed into seven groups (n=8): Arthritis induced and untreated (ZY); Arthritis induced and treated with dexamethasone (ZY + DEXA); Arthritis induced and treated with LLLT at 3 Jcm^{-2} energy density (ZY + 3 Jcm^{-2}); Arthritis induced and treated with LLLT at 30 Jcm^{-2} energy density (ZY + 30 Jcm^{-2}); Euthanized 5h after arthritis induction (5h) and control group (C).

The arthritis induction was performed as previously described by Dimitrova et al. (DIMITROVA et al., 2010). Briefly, a solution containing 180µg of zymosan A from *Saccharomyces cerevisiae* (Sigma Chemical Company, USA) dissolved in 10µL of sterile phosphate buffer solution (PBS) was injected into the region near talocrural and subtalar joints (right and left) of mouse hind limbs. To the control group, only 10µL of sterile PBS solution was administrated. All procedures were performed using anesthesia: a mix of 80mg kg^{-1} ketamine (Syntec, Brazil) and 20mg kg^{-1} xylazine (Syntec, Brazil) by intraperitoneal via. In order to confirm the beginning of inflammation process and the best moment to treatments beginning, a group was created and euthanized 5 hours after arthritis induction (Ankle joint photomicrographs of control and 5h groups as well as the morphological methods are available on supplementary material).

LLLT and dexamethasone protocols

A gallium-aluminum-arsenide (GaAlAs) low-level infrared laser (HTM Indústria de Equipamentos Eletroeletrônicos Ltda, Brazil) was used in the following parameters: continuous wave emission mode, 830nm wavelength, 10mW power output, 0.05cm^2 spot area, irradiance at 0.2Wcm^{-2}, energy

densities at 3 and 30 Jcm^{-2} (total energy of 150 and 1500mJ were delivered after 15 and 150s, respectively). Laser irradiation was applied at one point on ankle joint (medial and external side of the ankle) and the optical pen was positioned perpendicularly to the skin. The dexamethasone (Aché Pharmaceutical Laboratory, Brazil) was administrated by intraperitoneal via (4 $mg\ kg^{-1}$).

The LLLT and dexamethasone administration were performed 4 times: 5, 29, 53, and 77h after zymosan administration. Twenty-four hours after the last treatment section (101h / 4 days after zymosan administration), the groups were euthanized. Their ankles together with a tiny portion of structures above and below of ankle, as muscles and bones, were removed and the skin were dissected (right ankles were used for cytokines measurement by ELISA and the left ankle for real-time PCR) as well as the both proximal lymph nodes (popliteal) were used for flow cytometry analysis.

Quantification of cytokines mRNA relative levels by real-time quantitative polymerase chain reaction assay (qRT-PCR)

Total RNA was isolated from left hide ankle after maceration with liquid nitrogen, using cold Trizol Reagent (Invitrogen, USA) according to the manufacturer's instructions. Then, 2µg of total RNA were transcribed to complementary DNA (cDNA) using the High-Capacity cDNA Reverse Transcription Kit (Applied Biosystems, USA). The primers for qRT-PCR were designed using the Primer 3 program (UNTERGASSER et al., 2012), on different exons in order to avoid the possibility of genomic DNA contamination. The primers of genes used here (encoding the cytokines IL-1β, IL-6, IL-10, TNF-α and TGF-β) are described in supplementary material (Table S1) as well as of β-actin, used as internal control. qRT-PCR assay was performed in StepOnePlus™ Real-Time PCR System instrument (Applied Biosystems, USA).

For gene relative levels analysis by qRT-PCR the Delta-Delta Ct method (ΔΔCt) was used (LIVAK & SCHMITTGEN, 2001). Internal normalization was performed by β-actin and untreated samples (ZY) were used to calculate the ΔΔCt.

Quantification of cytokines extracted from arthritic ankle

After skin dissection, total proteins was extracted from hide right ankles using 100mg of tissue/ml in PBS buffer supplemented with 0.4MNaCl, 0.05% Tween 20 and protease inhibitors (0.1mM PMSF, 0.1mM benzethonium chloride, 10mM EDTA and 20KI aprotinin A / 100ml). The samples were macerated, homogenized and centrifuged for 15min at 10,000rpm (4ºC). The levels of IL-1β, IL-6 and TNF-α and IL-10 were estimated using a commercially available ELISA (enzyme-linked immunosorbent assay) kit (BD Biosciences, USA) according to the manufacturer's guidelines. The plates were read using a 450nm wavelength laser. The optical density was analyzed and a standard curve was constructed using SoftMax® Pro software (Molecular devices, USA).

Flow Cytometry of immune cells in lymph node proximal to inflammation (popliteal)

Multicolour flow cytometry was used to identify the popliteal lymph node cells and expression of cell surface markers. All monoclonal antibodies (mAbs) were obtained from BD Biosciences (USA): anti-CD11b, anti-CD11c, anti-CD80, anti-CD86, anti-CD3, anti-NK1.1, anti-CD4, anti-CD8, anti-CD25 and anti-FoxP3. In brief, after the both rear popliteal lymph node removal from each animals, the maceration were performed joining lymph nodes of 2 animals. The cells were counted in Neubauer's Chamber and plated at 10^6 per well. To extracellular labeling the cells were washed twice in staining buffer and then stained for 30 minutes at 4°C with antibodies fluorochrome-labeled. To intracellular staining, cells were stained for cell surface markers for 30 minutes at 4°C with antibodies fluorochrome-labeled and then fixed and permeabilized with the FoxP3 buffer set (BD Biosciences) according to the manufacturer's instructions and stained with antibody anti-FoxP3. Flow cytometry data were acquired on a FACsCanto ™ II (BD Biosciences) and analyzed with FlowJo software (version 10). The mean fluorescence intensity (MFI) were determined to CD80, CD86 and CD25.

Statistical analysis

Statistical analyses were performed using GraphPad Prism 7.04 (GraphPad Software Inc., USA). Data are presented as means ± SD. Multiple comparisons were performed using the one-way ANOVA tests followed by Bonferroni multiple contrast hypothesis test. P values less than 0.05 were considered significant.

Results

Morphological analysis

The arthritis was successfully induced in mouse subtalar and talocrural joints. The inflammation was characterized by influx of polymorphonuclear cells (PMN), particularly neutrophils in synovial tissues and their adjacent connective tissues 5 hours after zymosan injection (Figure S1). This inflammation was also characterized for an intense pro-inflammatory cytokine gene expression if compared to untreated group (Figure S2). At this moment, we started the treatments protocols: ZY + 3 Jcm^{-2}, ZY + 30 Jcm^{-2} and ZY + DEXA groups.

The inflammation process persisted until the fourth day for the untreated group. Macrophages, lymphocytes and intense fibrous tissue deposition could also be observed. The control group showed ankle joint normal histological features (Figure S1).

Cytokines levels

The cytokines mRNA relative levels are shown in the Figure 1. ZY + 3 Jcm^{-2} and ZY + DEXA groups demonstrated IL-1β mRNA relative levels reduced when comparing to ZY (ZY + 3 Jcm^{-2} $p<0.0001$; ZY + DEXA $p<0.0001$) and ZY + 30 Jcm^{-2} groups (ZY + 3 Jcm^{-2} $p<0.0001$; ZY + DEXA $p<0.0001$). Meanwhile, ZY + 30 Jcm^{-2} group showed IL-1β mRNA relative levels reduced comparing to ZY group ($p=0.0124$) (Figure 1A). Figure 1B shows IL-6 mRNA

relative levels reduced for ZY + 3 Jcm^{-2} and ZY + DEXA groups when compared to ZY (ZY + 3 Jcm^{-2} p=0.0031; ZY + DEXA p=0.0018) and ZY + 30 Jcm^{-2} groups (ZY + 3 Jcm^{-2} p<0.0001; ZY + DEXA p<0.0001); differently, ZY + 30 Jcm^{-2} group showed a increase levels when compared to ZY group (p<0.0001). Figures 1C, 1D and 1E show mRNA relative levels of TNF-α, IL-10 and TGF-β, respectively. For these analysis, ZY + 3 Jcm^{-2} group presented higher levels than all others groups (Compared to ZY: TNF-α p=0.0008, IL-10 p<0.0001 and TGF-β p=0.0042; Compared to ZY + 30 Jcm^{-2}: TNF-α p<0.0001, IL-10 p<0.0001 and TGF-β p=0.0120; Compared to ZY + DEXA: TNF-α p<0.0001, IL-10 p<0.0001 and TGF-β p=0.0055).

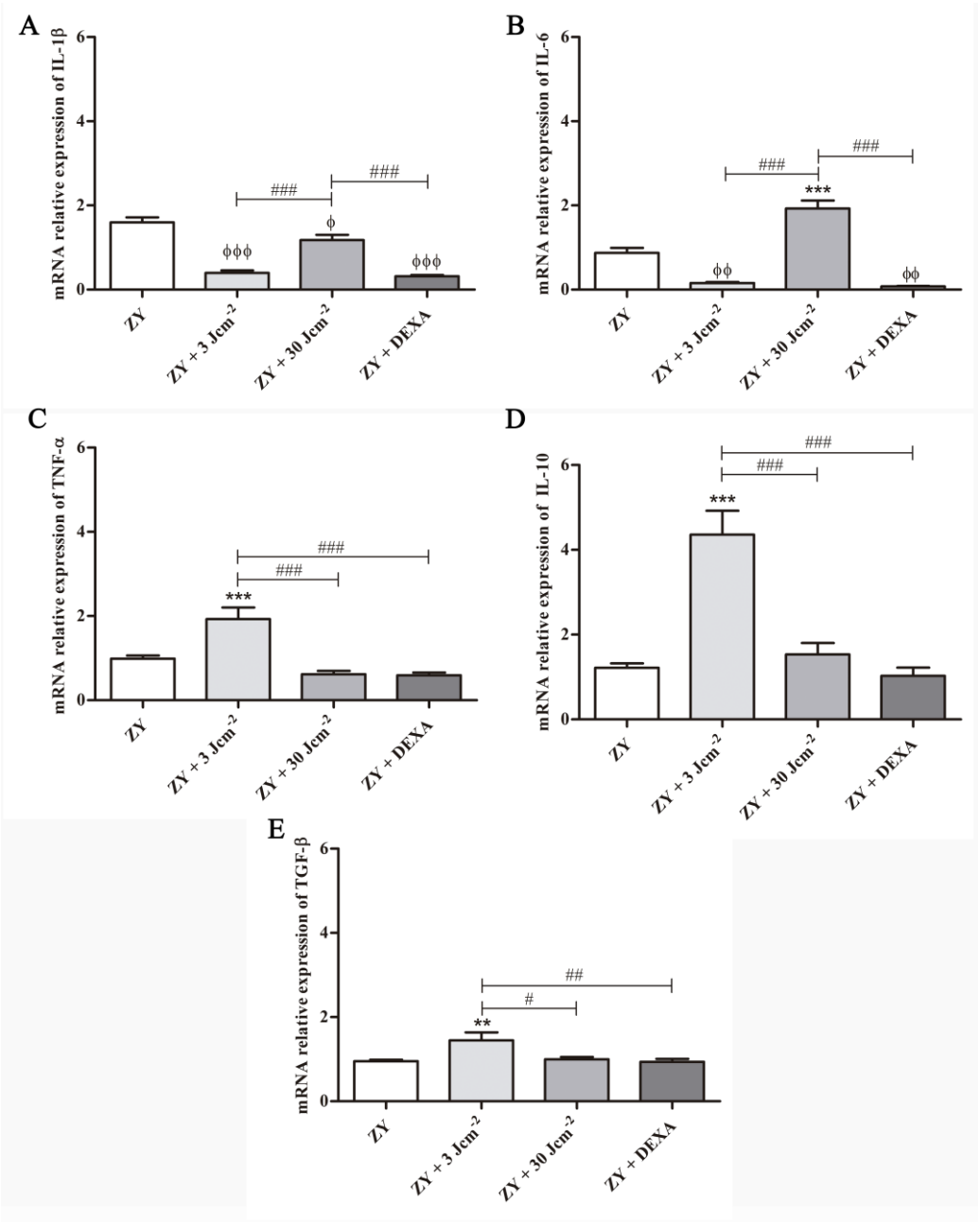

Figure 1 - Cytokines mRNA relative levels in mouse ankle joints after LLLT and dexamethasone treatments. **A:** IL-1 β; **B:** IL-6; **C:** TNF-α; **D:** IL-10; **E:** TGF:β. β-actin was used as an internal control. Untreated group - ZY, LLLT at 3 Jcm^{-2} (ZY + 3 Jcm^{-2}), LLLT at 30 Jcm^{-2} (ZY + 30 Jcm^{-2}) and treated with dexamethasone (ZY + DEXA) mice. (*) $p < 0.05$, (**) $p < 0.01$ and (***) $p < 0.001$ when compared to the untreated group (ZY). ($^{\phi}$) $p < 0.05$, ($^{\phi\phi}$) $p < 0.01$ and ($^{\phi\phi\phi}$) $p < 0.001$ when smaller than the untreated group (ZY). ($^{\#}$) $p < 0.05$, ($^{\#\#}$) $p < 0.01$ and ($^{\#\#\#}$) $p < 0.001$.

Levels of all cytokines were decreased after LLLT, when compared to untreated group: ZY + 3 Jcm^{-2} - IL1-β ($p=0.0039$), IL-6 ($p<0.0001$), IL-10 ($p<0.0001$) and TNF-α $p<0.0001$; ZY + 30 Jcm^{-2} - IL1-β ($p<0.0001$), IL-6 ($p<0.0001$), IL-10 ($p<0.0001$) and TNF-α ($p=0.0002$). The dexamethasone treated groups also demonstrated an important decrease in the levels of cytokines, when compared to untreated group: IL1-β ($p<0.0001$), IL-6 ($p=0.0009$), IL-10 ($p<0.0001$) and TNF-α ($p<0.0001$). On the other hand, this group showed higher level of IL-10 than ZY + 3 Jcm^{-2} ($p=0.0011$) (Figure 2).

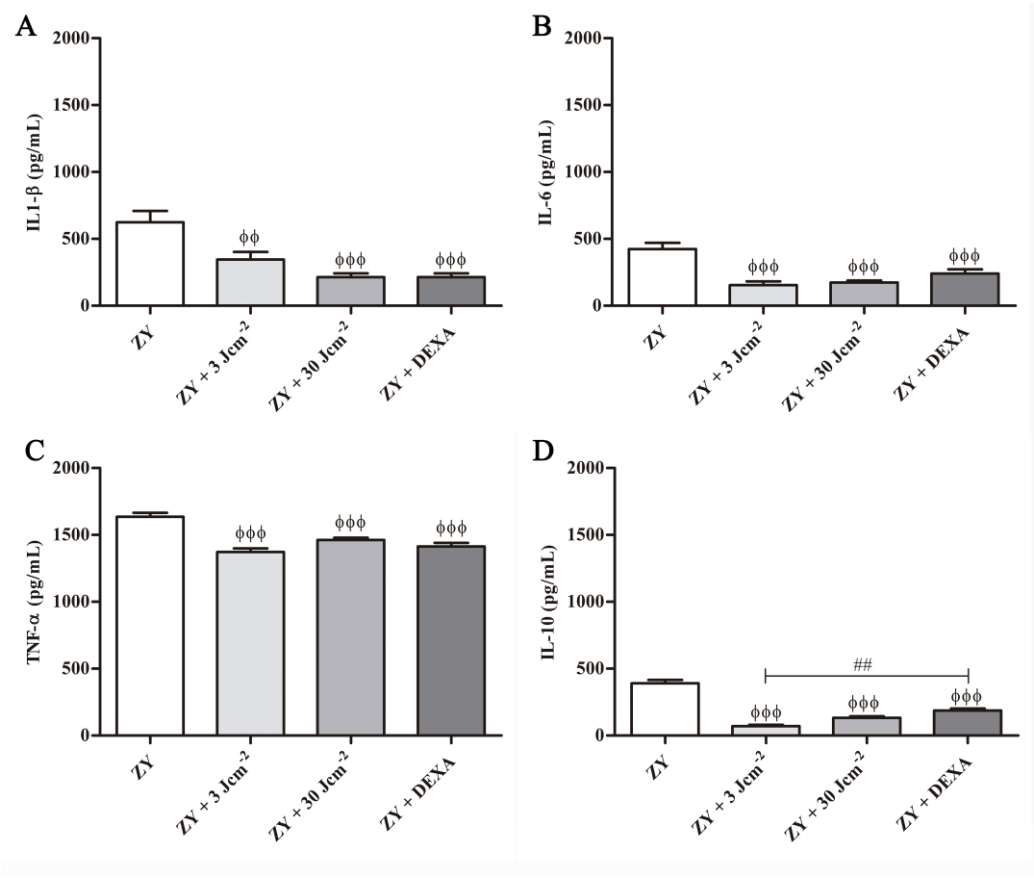

Figure 2 - Cytokines levels in mouse ankle joints after LLLT and dexamethasone treatments (pg/mL). **A:** IL-1β; **B:** IL-6; **C:** TNF-α; **D:** IL-10. Untreated group - ZY, LLLT at 3 Jcm^{-2} (ZY + 3 Jcm^{-2}), LLLT at 30 Jcm^{-2} (ZY + 30 Jcm^{-2}) and treated with dexamethasone (ZY + DEXA) mice. ($^{\phi\phi}$) $p < 0.01$ and ($^{\phi\phi\phi}$) $p < 0.001$ when compared to the untreated group (ZY). ($^{\#\#}$) $p < 0.01$.

Antigen-presentig cells quantification and profile

ZY + 3 Jcm^{-2} group demonstrated higher number of cells in lymph node (p=0.025) (Figure 3A) as well as macrophages ($CD11b^+$ cells) (p=0.0007) and DCs ($CD11c^+$ cells) (p=0.0024) population than ZY + DEXA group (Figure 3B and 3C). Among macrophage population, there were higher number of cells expressing costimulatory surface protein CD86 (p=0.0049) (Figure 3D) while for the DC population more cells expressing CD80 (p=0.0314) (Figure 3E). ZY + 3 Jcm^{-2} group also showed higher number of DCs expressing concomitantly CD80 and CD86 than ZY + DEXA (p=0.0185) and ZY (p=0.0240) groups (Figure 3F).

Likewise, ZY + 30 Jcm^{-2} group demonstrated higher number of cells in lymph node (p=0.0037) (Figure 3A) as well as macrophages population (p=0.0228) when compared to ZY + DEXA group (Figure 3B and 3C). Although their DC population rate was not statistically different from ZY + DEXA group (p=0.1745) (Figure 3B and 3C), there were more DCs expressing CD86 (p=0.0467) (Figure 3E). ZY + 30 Jcm^{-2} group also demonstrated higher quantity of CD80 expression on DCs surface than ZY group (p=0.0160) (Figure 3E). Furthermore, macrophages expressing concomitantly CD80 and CD86 were observed higher ZY + 30 Jcm^{-2} than ZY + DEXA (p=0.0298) (Figure 3F).

Effector cells of adaptive immune response profile

ZY + 3 Jcm^{-2} group showed higher NK cells rate than ZY + DEXA group (p=0.0330) (Figure 4A and 4B). Additionally, T helper ($CD4^+$), T cytotoxic ($CD8^+$) (Figure 4C and 4D) and Treg cells ($CD4^+FoxP3^+CD25^+$) rates were increased when compared to ZY ($CD4^+$ p=0.0449; $CD8^+$ p=0.0304; Treg p=0.0363) and ZY + DEXA ($CD4^+$ p=0.0088; $CD8^+$ p=0.0011; Treg p=0.0056) groups (Figure 4E and 4F) as well as the number of $CD4^+FoxP3^+CD25^{high}$ cells (Compared to ZY p=0.0108; compared to ZY + 30 Jcm^{-2} p=0.0185; compared to ZY + DEXA p=0.034) (Figure 4G and 4H). On the other hand, ZY + 30 Jcm^{-2} showed only $CD8^+$ cells rate increased when compared to ZY + DEXA group (p=0.0162) (Figure 4D).

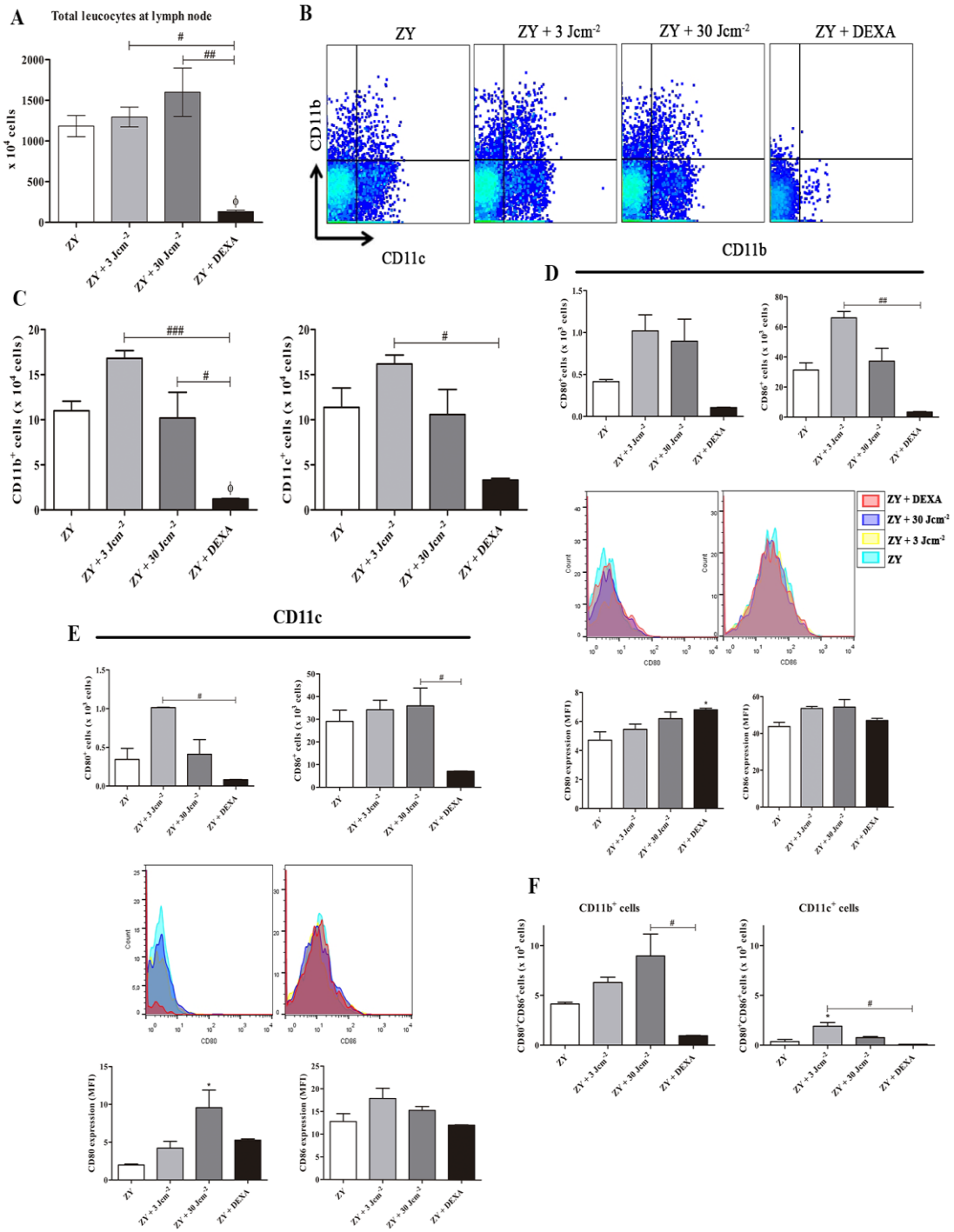

Figure 3 - Macrophages, dendritic cells and its costimulatory surface proteins in lymph node proximal to inflammation. **A**: Total cell; **B**: Representative flow cytometry plots show distribution of $CD11b^+$ cells and $CD11c^+$ cells for each group; **C**: $CD11b^+$ cells and $CD11c^+$ cells proportion; **D** and **E**: lymph node cells were gated on CD11b or CD11c expression and stained for CD80 and CD86 costimulatory surface proteins. Proportions of $CD11b^+CD80^+$cells/$CD11c^+CD80^+$cells and $CD11b^+CD86^+$cells/ $CD11c^+CD86^+$cells are shown for each group as well as the histograms of CD80 and CD86 expression and its levels by MFI; **F**: Proportions of $CD11b^+$ cells and $CD11c^+$ cells double positive to $CD80^+$ and $CD86^+$. Untreated group - ZY, LLLT at 3 Jcm^{-2} (ZY + 3 Jcm^{-2}), LLLT at 30 Jcm^{-2} (ZY + 30 Jcm^{-2}) and treated with dexamethasone (ZY + DEXA) mice.

(*) $p < 0.05$ when bigger than the untreated group (ZY). ($^{\phi}$) $p < 0.05$ when smaller than the untreated group (ZY). ($^{\#}$) $p < 0.05$, ($^{\#\#}$) $p<0.01$ and ($^{\#\#\#}$) $p < 0.001$.

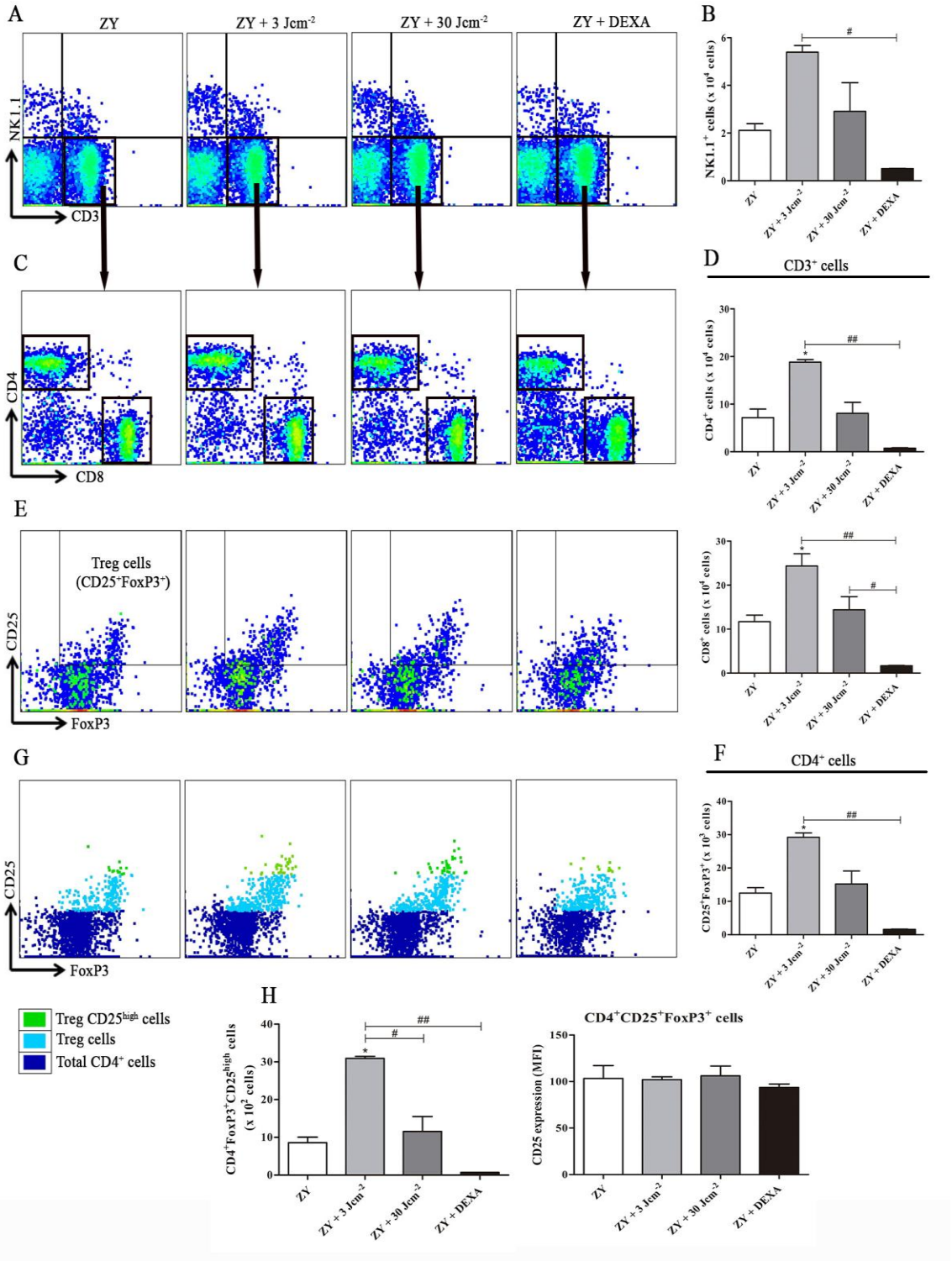

Figure 4 - NK cells and adaptive immune cells in lymph node proximal to inflammation. **A**, Representative flow cytometry plots show distribution of $CD3^+$ cells and $NK1.1^+$ cells from lymph node total leukocytes, for each group - ZY, LLLT at 3 Jcm^{-2} (ZY + 3 Jcm^{-2}), LLLT a 30 Jcm^{-2} (ZY + 30 Jcm^{-2}) and treated with dexamethasone (ZY + DEXA) mice. **B**, Proportions of $NK1.1^+$ cells for each group are shown. **C**, Representative flow cytometry plots show distribution of $CD4^+$

cells and $CD8^+$ cells from $CD3^+$ cells, for each group. **D,** Proportions of $CD4^+$ and $CD8^+$ cells for each group. **E**, Representative flow cytometry plots show distribution of $CD25^+$ cells and $FoxP3^+$ cells from $CD4^+$ cells and the double positive cells (Treg cells), for each group. **F**, Proportions of Treg cells ($CD4^+CD25^+FoxP3^+$) for each group. **G**, Representative flow cytometry plots show distribution of $CD25^+$ cells and $FoxP3^+$ cells from $CD4^+$ cells and the $CD25^{high}$ cells among the double positive cells (Treg cells), for each group. **H**, Proportions of $CD4^+$ $FoxP3^+$ $CD25^{high}$ and the level of CD25 expression by MFI, for each group. Untreated group - ZY, LLLT at 3 Jcm^{-2} (ZY + 3 Jcm^{-2}), LLLT at 30 Jcm^{-2} (ZY + 30 Jcm^{-2}) and treated with dexamethasone (ZY + DEXA) mice. (*) $p < 0.05$ if bigger than the untreated group (ZY). (ZY). ($^{\#}$) $p < 0.05$ and ($^{\#\#}$) $p<0.01$.

Discussion

In a previous work, we showed that LLLT promotes apoptosis in PMN cells at joint, which could comprise one of LLLT anti-inflammatory mechanisms (ANJOS et al., 2017). Due this fact, the present study investigated whether this treatment could also modify the immune response in the same arthritis experimental model.

Anti-inflammatory effects were observed after LLLT through changes in the pro- and anti-inflammatory cytokine mRNA relative levels and in the reduction of IL-1β, IL-6, IL-10 and TNF-α (Figures 1 and 2) at inflammation site. Also, LLLT at 3 Jcm^{-2} presented a tendency to maintain this anti-inflammatory profile at joint since IL-10 and TGF-β mRNA relative levels were higher than all others groups. Although the elevation in mRNA relative levels of the pro-inflammatory cytokines TNF-α and IL-6 were observed in the 3 Jcm^{-2} and 30 Jcm^{-2} groups, respectively, it does not necessarily mean a return to the pro-inflammatory state. Despite TNF-α is classically a pro-inflammatory cytokine, it is able to inhibit the function of mature DCs and also conduce to their apoptosis, resulting in antigen presentation failure and reducing lymphocytes levels by apoptosis (O'SHEA et al., 2002). More, recent researches have been shown that IL-6 presents pleiotropic functions in the acute phase response, inducing neutrophil apoptosis and switching from neutrophil to monocyte recruitment in inflammation site by suppressing mainly neutrophil-attracting chemokines (SCHELLER et al., 2011). These IL-6 effects substantially contribute to acute infiltration resolution, since neutrophils are the most abundant cells in our inflammation model (Figure S1).

LLLT has been presented an activity on inflammation by modulation of pro- and anti-inflammatory mediator expression, such as IL-1β, lL-6, TNF-α, TGF-β and lL-10 (ALVES et al., 2013; ASSIS et al., 2016; DOS SANTOS et al., 2014; FUKUDA et al., 2013; LUO et al., 2013; TORRES-SILVA et al., 2015), however the possible explanation to the LLLT cellular mechanisms that had driven to these results is poorly understood yet. It is known that the photobiological effects induced by LLLT are due to excitation of specific molecules, the so-called photoacceptors, by absorption of laser photons (EVANS & ABRAHAMSE, 2009), triggering the secondary messengers production (as reactive oxygen species - ROS, lymphokines, cytokines and nitric oxide - NO) capable to initiate a cascade of intracellular signals and initiate, inhibit or accelerate biological processes, such as wound healing and inflammation resolution (KARU, 1999; KARU, 2008).

Due to PMN cells additional mechanism for free radical production and their very short half-life during inflammation, LLLT might have greater and specific effects on these cells, accelerating the cellular functions, as cytokines production, and the consequent cell death by apoptosis [16, 33]. Since the inflammatory cells were exposed to repeated biostimulation in the LLLT treatment sections, it was expected that inflammatory cytokines profile was altered. In fact, the decrease of pro-inflammatory cytokines production, as observed after the intense elevation of its levels, agrees with the LLLT biphasic dose-response, as previously reported (HUANG et al., 2009), and the anti-inflammatory profile commonly found at the final stages of inflammatory process resolution (PERRETTI et al., 2017).

Once the expression of pro-inflammatory cytokines was increased in the inflammation induced by zymosan, in particular IL-1β, TNF-α and IL-6 (Figure S2), the reduction of cytokine levels presented in lasers-treated groups demonstrates the anti-inflammatory effect of phototherapy at low energy densities and its positive effects on arthritis treatment.

In our arthritis-induced model, the inflammatory response triggered by zymosan is linked to its phagocytosis, a process that is mediated by cell surface receptors. In the induction phase of immune response (sensitization or afferent phase), the phagocytes (monocytes, macrophages and dendritic cells)

recognize zymosan by receptor binding, resulting in the activation of NF-κB and the production of the inflammatory cytokines as well as the expression of the costimulatory molecule CD80. Additionally, zymosan is able to elicit adaptive immune responses through DC maturation and IL-12 production stimulation, leading to mature DCs migration to regional lymph nodes and induction of T lymphocytes activation as well as its proliferation through antigen (zymosan) presentation. In the elicitation (efferent) phase, repeated contact with zymosan induces recruitment of the T lymphocytes, which in turn produce a variety of cytokines, amplifying the background inflammatory response into a more vigorous process (FRASNELLI et al., 2005; GRANUCCI et al., 2003; KARUMUTHIL-MELETHIL et al., 2015; KEYSTONE et al., 1977). This intense pro-inflammatory microenvironment could be observed in non-treated group due to elevated levels of cytokines (Figures 2 and S2).

Differently, the dexamethasone treatment showed an important reduction in the cytokines levels (Figure 2) as well as in the number of all immune cells analyzed from lymph node proximal to inflammation (Figure 3A). These results were already expected, since corticosteroids, as dexamethasone, switch off multiple inflammatory genes (encoding cytokines, chemokines, adhesion molecules, inflammatory enzymes, receptors and proteins), which have been activated during inflammation, consequently decreasing pro-inflammatory cells and mediators in a non-specific manner (COUTINHO & CHAPMAN, 2011). As dexamethasone is commonly used for articular inflammatory treatments, as arthritis, the ZY + DEXA group results was used as a gold standard in the statistical analysis of LLLT groups flow cytometry date.

In view that T cell differentiation induction into $CD4^+$ or $CD8^+$ cells (cytotoxic T cells) subsets occurs through antigen presentation with MHC and the costimulatory proteins CD80/CD86 by DCs and macrophages (MCINNES & SCHETT, 2011), there were greater antigen presentation at lymph node of group treated with LLLT at 3 Jcm^{-2} group once macrophage and DCs population as well as the number of costimulatory surface proteins expressed on macrophages (CD86) and on DCs (either only CD80 or both CD80/CD86, concomitantly) presented increase. The macrophages and DCs elevated rates also suggest an increase in the cytokine milieu at lymph node. Both results are

crucial to activation and clonal expansion of lymphocytes (MCINNES & SCHETT, 2007), as observed in the rates of lymphocytes subsets, $CD4^{+,}$ $CD8^{+}$ and Treg cells of LLLT + 3 Jcm^{-2} group. The increased T cells populations, particularly $CD4^{+}$ subsets, and its cytokines and chemokines production promote a positive feedback loops on inflammation leading to RA synovitis chronicity (CHOY, 2012). The same way, the costimulatory proteins present an important role in the RA pathophysiology, proven by Abatacept drug treatment efficacy, which promotes impair of antigen presentation to T cells by blocking T-cell costimulation (through the interaction of CD28 with CD80 or CD86) (CANTAERT et al., 2009).

This study is the first that shows Treg enrichment after LLLT (increased Treg rate in the LLLT + 3 Jcm^{-2} group). Moreover, it is demonstrated a number of Treg cells expressing higher levels of CD25 (receptor of IL-2 on cell surface of Treg), important marker to its regulatory potency (BAECHER-ALLAN et al., 2001). Thus, Treg cells population increase, especially presenting $CD4^{+}FoxP3^{+}CD25^{high}$ phenotype, induced by laser at 3 Jcm^{-2} could favor the negative modulation of the immune response in the inflammatory microenvironment leading to inflammation resolution. In fact, Treg accumulation presenting activated phenotype represents positive factor in the prognosis of rheumatic disorders, once they are commonly associated with compromised Treg function (MORADI et al., 2014; RAGHAVAN et al., 2009), and in some patients the successful treatment of RA are related to the reversion on Treg effector function (COOLES et al., 2013).

LLLT at the lower fluence was also able to induce the higher rate of NK cells. These cells are commonly expanded in inflamed joints and are responsible for pro-inflammatory cytokines production amplification, interacting with the macrophage/monocyte population infiltrating the joint (DALBETH & CALLAN, 2002).

On the other hand, the group treated with LLLT at 30 Jcm^{-2} showed lesser changes in the immune cells profile in lymph node proximal to inflammation. Although the lymph node hyperplasia was observed in this group, only macrophage (Figure 3) and $CD8^{+}$ cells (Figure 4) populations were increased, besides a greater expression of costimulatory proteins on

macrophages and DCs (Figure 3). Thus, in this group the antigen presentation by macrophages expanded or DC expressing more costimulatory proteins seems to induce $CD8^+$ profile on lymph node T cells.

The different results of the two energy densities seem to be related to biostimulation promoted by them. Since the irradiation is more intense at 30 Jcm^{-2}, it is plausible conclude that cell effects from this treatment would be more pronounced than those observed at 3 Jcm^{-2}. However, the biochemical mechanisms underlying the LLLT positive effects on inflammation commonly shown a biphasic dose-response: cell activation is limited and, after achieves its threshold, it is followed by the consequent cellular activity reduction and possible the cell death (HUANG et al., 2009). Keeping this in mind, the lower changes in the profile of lymph node immune cells observed in the group treated with LLLT at 30 Jcm^{-2} could be a repercussion of the intense photobiostimulation promoted by this therapy, which accelerates the cellular activities leading to a faster inflammation resolution. Thus, the immune cells population observed in the group treated with LLLT at 30 Jcm^{-2} could indicate the lymph node cells profile at final stages of inflammation resolution when also phagocytosis of polymorphonuclear (PMN) apoptotic cells by macrophages and the contraction of lymphocytes population are observed (PERRETTI et al., 2017; SAVILL et al., 2002). This hypothesis is corroborated by our previously study, which reports an important anti-inflammatory effect of LLLT at 30 Jcm^{-2} through the photobiostimulation and consequent PMN cells apoptosis induction at arthritic site. This anti-inflammatory effect was not observed in the group treated with LLLT at 3 Jcm^{-2}, although a tendency to PMN cell apoptosis induction was observed (ANJOS et al., 2017).

The changes in the immune cell profile after LLLT on lymph node proximal to inflammation, with increase of antigen presentation to T cells and its clonal expansion, could be attributed to lymphangiogenesis and lymphatic motility stimulation LLLT capabilities (LAU & CHEING, 2009) and both can contribute to immune cells migration from joint to lymph node (or in the opposite direction).

Once the development of new treatments for inflammation, that reach an effective anti-inflammatory behavior without deleterious effect on immune

system, is an important challenge (O'NEILL, 2006), the LLLT presents promising potential, since demonstrated be able to reduce the pro-inflammatory cytokine levels in the inflammation site and induce changes in T cell populations at lymph node (including Treg cells increasing), differently of the non-specific immune system depression induced by dexamethasone treatment.

Conclusion

LLLT anti-inflammatory effect, reported in experimental and clinical studies, have been mainly attributed to inflammation mediator modulation. Furthermore, we showed that there are alterations in the populations of antigen-presenting cells, lymphocytes and Treg cells expressing CD25 at high levels in proximal lymph node to inflammation. Taken together our results indicate that LLLT is an alternative for treatment of rheumatic disorders since is able to change the inflammatory course of arthritis, tending to accelerate its resolution through immune cells photobiostimulation.

Acknowledgements

We thank to Brazilian funding agencies FAPEMIG **(**#APQ 02123/15) and CNPq (#474405/2013-3) for the financial support of this research. The authors would like to thank Dr. Gilson Costa Macedo for his help in the acquisition and interpretation of flow cytometry data.

Conflict of interest

No competing financial interests exist.

References

ALVES, A. C. et al. Effect of low-level laser therapy on the expression of inflammatory mediators and on neutrophils and macrophages in acute joint

inflammation. Arthritis Research & Therapy, v. 15, n. 5, p. R116, 2013.

ASIF AMIN, M.; FOX, D. A.; RUTH, J. H. Synovial cellular and molecular markers in rheumatoid arthritis. Seminars in Immunopathology, v. 39, n. 4, p. 385–393, 2017.

ASQUITH, D. L. et al. Animal models of rheumatoid arthritis. European Journal of Immunology, v. 39, n. 8, p. 2040–2044, 2009.

ASSIS, L. et al. Aerobic exercise training and low-level laser therapy modulate inflammatory response and degenerative process in an experimental model of knee osteoarthritis in rats. Osteoarthritis and Cartilage, v. 24, n. 1, p. 169–177, 2016.

BAECHER-ALLAN, C. et al. CD4+CD25high Regulatory Cells in Human Peripheral Blood. The Journal of Immunology, v. 167, n. 3, p. 1245–1253, 2001.
BROSSEAU, L. et al. Low level laser therapy (Classes I , II and III) for treating rheumatoid arthritis (Review). n. 4, 2010.

BURMESTER, G. R.; PRATT, A. G.; SCHERER, H. U.; VAN LAAR, J. M. Rheumatoid arthritis: pathogenesis and clinical features. In: EULAR textbook on Rheumatic Diseases. 1st edn ed. London: BMJ Publications, 2012. p. 206–231.
CANTAERT, T. et al. Alterations of the synovial T cell repertoire in anti-citrullinated protein antibody-positive rheumatoid arthritis. Arthritis and Rheumatism, v. 60, n. 7, p. 1944–1956, 2009.

CHOY, E. Understanding the dynamics: pathways involved in the pathogenesis of rheumatoid arthritis. Rheumatology, v. 51, n. suppl 5, p. v3–v11, 2012.

COOLES, F. A. H.; ISAACS, J. D.; ANDERSON, A. E. Treg cells in rheumatoid arthritis: An update. Current Rheumatology Reports, v. 15, n. 9, 2013.

COUTINHO, A. E.; CHAPMAN, K. E. The anti-inflammatory and

immunosuppressive effects of glucocorticoids, recent developments and mechanistic insights. Molecular and Cellular Endocrinology, v. 335, n. 1, p. 2–13, 2011.

CROSS, M. et al. The global burden of rheumatoid arthritis: Estimates from the Global Burden of Disease 2010 study. Annals of the Rheumatic Diseases, v. 73, n. 7, p. 1316–1322, 2014.

DALBETH, N.; CALLAN, M. F. C. A subset of natural killer cells is greatly expanded within inflamed joints. Arthritis and Rheumatism, v. 46, n. 7, p. 1763–1772, 2002.

DIMITROVA, P. et al. The role of properdin in murine zymosan-induced arthritis. Molecular Immunology, v. 47, n. 7–8, p. 1458–1466, 2010.

DOS ANJOS, L. M. J. et al. Apoptosis induced by low-level laser in polymorphonuclear cells of acute joint inflammation: comparative analysis of two energy densities. Lasers in Medical Science, v. 32, n. 5, p. 975–983, 2017.

DOS SANTOS, S. A. et al. Comparative analysis of two low-level laser doses on the expression of inflammatory mediators and on neutrophils and macrophages in acute joint inflammation. Lasers in Medical Science, v. 29, n. 3, p. 1051–1058, 2014.

EVANS, D. H.; ABRAHAMSE, H. A review of laboratory-based methods to investigate second messengers in low-level laser therapy (LLLT). Medical Laser Application, v. 24, n. 3, p. 201–215, 2009.

FIRESTEIN, G. S. Evolving concepts of rheumatoid arthritis. Nature, v. 423, n. 6937, p. 356–361, 2003.

FRASNELLI, M. E. et al. TLR2 modulates inflammation in zymosan-induced arthritis in mice. Arthritis research & therapy, v. 7, n. 2, p. R370-9, 2005.

FUKUDA, T. Y. et al. Infrared low-level diode laser on inflammatory process modulation in mice: Pro- and anti-inflammatory cytokines. Lasers in Medical Science, v. 28, n. 5, p. 1305–1313, 2013.

GRANUCCI, F. et al. Early IL-2 production by mouse dendritic cells is the result of microbial-induced priming. Journal of immunology (Baltimore, Md. : 1950), v. 170, p. 5075–5081, 2003.

HAQUE, M. et al. Utilizing Regulatory T Cells Against Rheumatoid Arthritis. Frontiers in Oncology, v. 4, n. August, p. 1–9, 2014.

HUANG, Y.-Y. et al. Biphasic Dose Response in Low Level Light Therapy. Dose-Response, v. 7, n. 4, p. dose-response.0, 2009.

IDE, M. R. et al. Functional capacity in rheumatoid arthritis patients: Comparison between Spanish and Brazilian sample. Rheumatology International, v. 31, n. 2, p. 221–226, 2011.

KARU, T. Primary and secondary mechanisms of action of visible to near-IR radiation on cells. Journal of Photochemistry and Photobiology B: Biology, v. 49, n. 1, p. 1–17, 1999.

KARU, T. I. Mitochondrial signaling in mammalian cells activated by red and near-IR radiation. Photochemistry and Photobiology, v. 84, n. 5, p. 1091–1099, 2008.

KARUMUTHIL-MELETHIL, S. et al. TLR2-and dectin 1-associated innate immune response modulates T-cell response to pancreatic β-cell antigen and prevents type 1 diabetes. Diabetes, v. 64, n. 4, p. 1341–1357, 2015.

KAZEM SHAKOURI, S. et al. Effect of low-level laser therapy on the fracture healing process. Lasers in Medical Science, v. 25, n. 1, p. 73–77, 2010.

KEYSTONE, E. et al. Zymosan-Induced Arthritis: A model of chronic proliferative arthritis following activation of the alternative pathway of complement. Arthritis & Rheumatism, v. 20, n. 7, p. 1396–1401, 1977.

KIELY, P. D. W. et al. Contemporary treatment principles for early rheumatoid arthritis: a consensus statement. Rheumatology, v. 48, n. 7, p. 765–772, 2009.
KINGSLEY J. D., D. T. AND M. R. Low-level laser therapy as a treatment for chronic pain. Frontiers in Phisiology, v. 5, n. 306, 2014.

LAU, R. W. L.; CHEING, G. L. Y. Managing Postmastectomy Lymphedema with Low-Level Laser Therapy. Photomedicine and Laser Surgery, v. 27, n. 5, p. 763–769, 2009.

LIVAK, K. J.; SCHMITTGEN, T. D. Analysis of relative gene expression data using real-time quantitative PCR and the 2-ΔΔCT method. Methods, v. 25, n. 4, p. 402–408, 2001.

LUO, L. et al. Effects of low-level laser therapy on ROS homeostasis and expression of IGF-1 and TGF-β1 in skeletal muscle during the repair process. Lasers in Medical Science, v. 28, n. 3, p. 725–734, 2013.

MAHDI, H. et al. Specific interaction between genotype, smoking and autoimmunity to citrullinated α-enolase in the etiology of rheumatoid arthritis. Nature Genetics, v. 41, n. 12, p. 1319–1324, 2009.

MCINNES, I. The Pathogenesis of Rheumatoid Arthritis. The new england journal of medicine, v. 365, n. 8, p. 2205–19, 2011.

MCINNES, I. B.; SCHETT, G. Cytokines in the pathogenesis of rheumatoid arthritis. Nature Reviews Immunology, v. 7, n. 6, p. 429–442, 2007.

MORADI, B. et al. CD4+CD25+/highCD127low/- regulatory T cells are enriched in rheumatoid arthritis and osteoarthritis joints-analysis of frequency and

phenotype in synovial membrane, synovial fluid and peripheral blood. Arthritis Research and Therapy, v. 16, n. 2, 2014.

NISHIMOTO, N.; KISHIMOTO, T. Interleukin 6: From bench to bedside. Nature Clinical Practice Rheumatology, v. 2, n. 11, p. 619–626, 2006.

O'NEILL, L. A. J. Targeting signal transduction as a strategy to treat inflammatory diseases. Nature Reviews Drug Discovery, v. 5, n. 7, p. 549–563, 2006.

O'SHEA, J. J.; MA, A.; LIPSKY, P. Cytokines and Autoimmunity. Nature Reviews Immunology, v. 2, n. 1, p. 37–45, 2002.

PERRETTI, M. et al. Immune resolution mechanisms in inflammatory arthritis. Nature Reviews Rheumatology, v. 13, n. 2, p. 87–99, 2017.

RAGHAVAN, S. et al. FOXP3 expression in blood, synovial fluid and synovial tissue during inflammatory arthritis and intra-articular corticosteroid treatment. Annals of the Rheumatic Diseases, v. 68, n. 12, p. 1908–1915, 2009.

SABEH, F.; FOX, D.; WEISS, S. J. Membrane-Type I Matrix Metalloproteinase-Dependent Regulation of Rheumatoid Arthritis Synoviocyte Function. The Journal of Immunology, v. 184, n. 11, p. 6396–6406, 2010.

SAVILL, J. et al. A blast from the past: Clearance of apoptotic cells regulates immune responses. Nature Reviews Immunology, v. 2, n. 12, p. 965–975, 2002.
SCHELLER, J. et al. The pro- and anti-inflammatory properties of the cytokine interleukin-6. Biochimica et Biophysica Acta - Molecular Cell Research, v. 1813, n. 5, p. 878–888, 2011.

SMOLEN, J. S. et al. EULAR recommendations for the management of rheumatoid arthritis with synthetic and biological disease-modifying antirheumatic drugs: 2016 update. Annals of the Rheumatic Diseases, v. 76, n.

6, p. 960–977, 2017.

SZEKANECZ, Z. et al. Chemokines and angiogenesis in rheumatoid arthritis. Frontiers in bioscience (Elite edition), v. 1, p. 44–51, 2009.

TORRES-SILVA, R. et al. The low level laser therapy (LLLT) operating in 660 nm reduce gene expression of inflammatory mediators in the experimental model of collagenase-induced rat tendinitis. Lasers in Medical Science, v. 30, n. 7, p. 1985–1990, 2015.

UNTERGASSER, A. et al. Primer3-new capabilities and interfaces. Nucleic Acids Research, v. 40, n. 15, p. 1–12, 2012.